Available online at www.sciencedirect.com
ScienceDirect
Journal of the European Ceramic Society 28 (2008) 1931–1939
www.elsevier.com/locate/jeurceramsoc

A further report on finite element analysis of sintering deformation using densification data—Error estimation and constrained sintering

Ruoyu Huang, Jingzhe Pan *

Department of Engineering, University of Leicester, Leicester LE1 7RH, UK

Received 30 August 2007; received in revised form 20 December 2007; accepted 4 January 2008
Available online 4 March 2008

Abstract

In a previous paper, Kiani et al. [Kiani, S., Pan, J., Yeomans, J. A., Barriere, M. B. and Blanchart, P., Finite element analysis of sintering deformation using densification data instead of a constitutive law. J. Eur. Ceram. Soc., 2007, **27**, 2377–2383] proposed an empirical numerical method to calculate the sintering deformation of ceramic powder compacts without knowing the viscosities and sintering potential. The method was validated by free sintering experiments using specimens with non-uniform initial densities. Two new developments are reported in this paper: (a) a method of error estimation is developed which can be used to check if the empirical analysis is valid after the analysis; (b) a range of case studies are presented showing that the empirical solutions provide very good approximations to the solutions obtained using full constitutive laws not only for free sintering but also for highly constrained sintering of single- or multi-layered films.

Keywords: Constrained sintering; Modelling; Finite element method; Sintering

1. Introduction

A modelling capacity to predict the sintering deformation of ceramic powder compacts is very important to ceramic manufacture. In theory, the finite element method (FEM) can be used to calculate the sintering deformation. In practice, the method has not been used very much by the ceramic industry for a very simple reason—it is often more time consuming and expensive to obtain the material data required by a finite element analysis than to develop a product using the trial-and-error approach. Just as an elastic stress analysis needs to know Young's modulus and Poisson's ratio of the material, a finite element analysis of the sintering deformation requires the shear and bulk viscosities of the powder compact as the input, which are defined through a so-called constitutive law:

$$\dot{\varepsilon}_{ij} = \frac{s_{ij}}{2\eta_S} + \frac{\sigma_m}{3\eta_B}\delta_{ij} + \dot{\varepsilon}_{exp}\delta_{ij}, \quad (1)$$

in which $\dot{\varepsilon}_{ij}$ is the strain rate, s_{ij} and σ_m are the deviatoric and mean stresses, δ_{ij} is the Kronecker delta function, η_S and η_B are the shear and bulk viscosities, and $\dot{\varepsilon}_{exp}$ is the free shrinking rate of a uniform powder compact when it is unconstrained and unstressed. The simplicity of Eq. (1) is deceiving because the two viscosities are strong functions of temperature, density and grain-size, all of which change dramatically during the sintering process. There are two approaches to establish the dependence of the viscosities on the microstructure: (a) using a material model; (b) directly fitting the experimental data. The predictions by the various material models are so diverse that it is very difficult to know which one to use.[1] Directly measuring the viscosities has been done by several research groups. For example, Bouvard's group at Grenoble developed a dilatometer-based technique [2–4] while Raether's group at Wurzburg developed an optical-based technique.[5] The measurement is however full of pitfalls. A force has to be applied to the fragile sample at elevated temperature. This very force can alter the microstructure and lead to a viscosity of an unwanted microstructure.

In a previous paper, Kiani et al. [6] showed that it is possible to calculate the sintering deformation without knowing the shear and bulk viscosities. They showed that a finite element solution to the following problem:

$$\int_V (\dot{\varepsilon}_{ij} - \dot{\varepsilon}_{exp}\delta_{ij})\,\delta\dot{\varepsilon}_{ij}\,dV = 0, \quad (2)$$

* Corresponding author. Tel.: +44 116 223 1092; fax: +44 116 252 2525.
E-mail address: jp165@le.ac.uk (J. Pan).

0955-2219/$ – see front matter © 2008 Elsevier Ltd. All rights reserved.
doi:10.1016/j.jeurceramsoc.2008.01.016

subjected to the boundary conditions provides a very good approximation to the full solution. Here $\delta\dot{\varepsilon}_{ij}$ represents the virtual variation of the strain rate. The integration is over the entire volume of the sintering body, V, which is known as the current configuration distinguished from V_0, known as the initial volume of the green body. In later discussions, this method is referred to as the densification-based finite element method or DFEM. The only material data required by the DFEM is the free shrinking rate of the material, $\dot{\varepsilon}_{\text{exp}}$, which is relatively easier to obtain experimentally than the viscosities. Eq. (2) attempts to match the actual strain rates, $\dot{\varepsilon}_{ij}$, with the free shrinking rate, $\dot{\varepsilon}_{\text{exp}}$, and satisfy the equilibrium, compatibility and boundary conditions at the same time. Kiani et al. [6] validated the method by free sintering experiments using specimens with non-uniform initial densities. However as an empirical method the uncertainty that its prediction may or may not be valid for a particular case is a major concern. The first objective of this paper is to present a method to estimate the error of the empirical analysis. The error estimation provides a necessary condition for the validity of the DFEM, i.e., a large error means that the empirical calculation is definitely invalid. If the error is small, then one should trust the DFEM with the same confidence as one would do for a finite element analysis using a full constitutive law. The second purpose of this paper is to present a series of case studies for highly constrained sintering. Constrained sintering is a relatively new industrial practice which is being used to fabricate multi-layered ceramics, piezoelectric films and protective coatings. A single layer or several layers of powder material is applied onto a substrate using techniques like inkjet printing, sol–gel process or dip coating. The system is then placed under elevated temperatures to cause it to consolidate. During sintering, the porous layer or layers tend to shrink while being restricted by each other and by the substrate. Taking a multi-layered fuel cell as an example, it has a complex structure comprising several layers of different ceramic materials that have varying degrees of porosity. The central electrolyte layer needs to be impermeable to the fuel and oxidant gases. The outer layers, the cathode and the anode, and the associated current collecting layers, need to be porous to allow the gases to reach their respective interfaces with the electrolyte and react. It is very important to control the sintering process so that the correct porosity is achieved for each layer and to ensure that the system is crack free. Because too many variables are involved in such sophisticated systems, it is very difficult to optimize the material and processing parameters using trial-and-error experiment. On the other hand it is practically unattainable to obtain full constitutive laws for each layer of different ceramic powders in order to carry out a finite element analysis. For such systems, the empirical method presented here provides an effective means for a proof of concept analysis.

2. Error estimation for the DFEM

The DFEM is a reduced format of the standard finite element method. The validity of the DFEM can be checked by comparing the predictions by the DFEM using Eq. (2) with those by the FEM using a full constitutive law (Eq. (1)) as reported by Kiani et al.[6] However, this comparison assumes that a full constitutive law with all its parameters is available. The purpose here is to develop a method of *posteriori* error estimation so that one can judge if a DFEM solution is valid or not without knowing the constitutive law.

The linear constitutive law of Eq. (1) can be re-written into an inverse form:

$$\sigma_{ij} = \lambda\dot{\varepsilon}_{kk}\delta_{ij} + 2\eta_{\text{S}}\dot{\varepsilon}_{ij} - 3\eta_{\text{B}}\dot{\varepsilon}_{\text{exp}}\delta_{ij} \tag{3}$$

in which $\lambda = \eta_{\text{B}} - 2\eta_{\text{S}}/3$, known as Lame constant, and $\dot{\varepsilon}_{kk}$ is the volumetric strain rate. When no external force is applied, the virtual power principle states that

$$\int_V \sigma_{ij}\delta\dot{\varepsilon}_{ij}\,\mathrm{d}V = 0. \tag{4}$$

Substituting Eq. (3) into Eq. (4) gives

$$\int_V 2\eta_{\text{S}}(\dot{\varepsilon}_{ij}-\dot{\varepsilon}_{\text{exp}}\delta_{ij})\,\delta\dot{\varepsilon}_{ij}\,\mathrm{d}V + \int_V \lambda(\dot{\varepsilon}_{kk}-3\dot{\varepsilon}_{\text{exp}})\,\delta\dot{\varepsilon}_{kk}\,\mathrm{d}V = 0, \tag{5}$$

which can be rewritten into a similar format as that given by Eq. (2):

$$\int_V 2\eta_{\text{S}}\,(\dot{\varepsilon}_{ij} - \dot{\tilde{\varepsilon}}_{\text{exp}}\delta_{ij})\,\delta\dot{\varepsilon}_{ij}\,\mathrm{d}V = 0 \tag{6}$$

in which

$$\dot{\tilde{\varepsilon}}_{\text{exp}} = (1-\zeta)\dot{\varepsilon}_{\text{exp}}, \tag{7}$$

where

$$\zeta = \frac{3\lambda}{2\eta_{\text{S}}}\frac{\dot{\varepsilon}_{kk} - 3\dot{\varepsilon}_{\text{exp}}}{3\dot{\varepsilon}_{\text{exp}}}. \tag{8}$$

In the empirical method η_{s} in Eq. (6) is assumed to be uniform over the entire sintering body. Under this assumption, if either $\lambda = 0$ or $\dot{\varepsilon}_{kk} = 3\dot{\varepsilon}_{\text{exp}}$, then $\zeta = 0$ and the DFEM formulation of Eq. (2) would be exactly valid. This strict condition can be relaxed into an integration form:

$$e_{\text{ave}}(t) = \frac{1}{t}\int_0^t \left(\frac{1}{V}\int_V |\zeta|\,\mathrm{d}V\right)\mathrm{d}t' \approx 0. \tag{9}$$

If the above condition is invalid but ζ is more or less uniform inside V at each time step, then the velocity field predicted by the DFEM would differ from that predicted by Eq. (1) by a scaling factor. In this case the DFEM and the FEM with a full constitutive law still predict the same final deformation although there will be a time lag between the two solutions. Therefore a condition for the DFEM to predict the correct final deformation can be given as

$$e_{\text{var}}(t) = \frac{1}{t}\int_0^t \left[\frac{1}{V}\int_V \left(\zeta - \frac{1}{V}\int_V \zeta\,\mathrm{d}V\right)^2 \mathrm{d}V\right]\mathrm{d}t' \approx 0. \tag{10}$$

When using DFEM, λ and η_{s} are unknown hence there is a problem to evaluate the integrations (9) and (10). Considering two frequent cases of constrained sintering in a three-dimensional Cartesian coordinate system: in case 1 the material is constrained only in one direction and free to sinter in the other two perpendicular directions (i.e., $\dot{\varepsilon}_{11} = 0$ and $\sigma_{22} = \sigma_{33} = 0$) and in case 2

the material is constrained in two perpendicular directions and free to sinter in the remaining direction (i.e., $\dot{\varepsilon}_{11} = \dot{\varepsilon}_{22} = 0$ and $\sigma_{33} = 0$). Using Eq. (3) the exact volumetric strain rate can be calculated as

$$\dot{\varepsilon}_{kk}^{\text{exact}} = \begin{cases} \dfrac{3 + 2(\eta_S/\lambda)}{1 + (\eta_S/\lambda)}\dot{\varepsilon}_{\text{exp}}, & \text{case 1} \\ \dfrac{3 + 2(\eta_S/\lambda)}{1 + 2(\eta_S/\lambda)}\dot{\varepsilon}_{\text{exp}}, & \text{case 2} \end{cases}, \tag{11}$$

while the DFEM gives

$$\dot{\varepsilon}_{kk}^{\text{DFEM}} = \begin{cases} 2\dot{\varepsilon}_{\text{exp}}, & \text{case 1} \\ \dot{\varepsilon}_{\text{exp}}, & \text{case 2} \end{cases}. \tag{12}$$

The DFEM would be exactly correct if λ is very small. If λ is not small, it can be shown that

$$\dot{\varepsilon}_{kk}^{\text{exact}} - 3\dot{\varepsilon}_{\text{exp}} \approx \text{Dim}\,\frac{\eta_S}{\lambda}\left(\dot{\varepsilon}_{kk}^{\text{DFEM}} - 3\dot{\varepsilon}_{\text{exp}}\right) \tag{13}$$

in which

$$\text{Dim} = \begin{cases} 1, & \text{case 1} \\ 2, & \text{case 2} \end{cases}. \tag{14}$$

Substituting Eq. (13) into Eq. (8) gives

$$\zeta \approx \text{Dim}\,\frac{3}{2}\frac{\dot{\varepsilon}_{kk}^{\text{DFEM}} - 3\dot{\varepsilon}_{\text{exp}}}{3\dot{\varepsilon}_{\text{exp}}}. \tag{15}$$

In a general case of constrained sintering, the actual constraint condition is close to either case 1 or case 2 according to the principle values (eigen values) of $\dot{\varepsilon}_{ij}^{\text{DFEM}}$. If a principle value of $\dot{\varepsilon}_{ij}^{\text{DFEM}}$ is much smaller than $\dot{\varepsilon}_{\text{exp}}$, then the corresponding direction of the principal strain rate should be considered as constrained. In fact we are only interested in whether any of the two integrations given by Eqs. (9) and (10) is close to zero. The expression for ζ given by Eq. (15) can be used in Eqs. (9) and (10) to determine if a DFEM calculation is (a) valid for the temporal evolution of the sintering deformation (if $e_{\text{ave}} \approx 0$), (b) valid for the final deformation (if $e_{\text{ave}} \gg 0$ but $e_{\text{var}} \approx 0$), or (c) completely invalid (if $e_{\text{ave}} \gg 0$ and $e_{\text{var}} \gg 0$).

3. Numerical case studies of DFEM

If a full constitutive law with all its parameters is available, then the free shrinking rate $\dot{\varepsilon}_{\text{exp}}$ can be calculated from the constitutive law. One way to test the DFEM is to compare the DFEM solution obtained using such calculated $\dot{\varepsilon}_{\text{exp}}$ with the finite element solution obtained using the full constitutive law. Such comparisons were made for free sintering cases by Kiani et al.[6] In the current paper, we present more case studies for constrained sintering. Two constitutive laws are used to test the DEFM for two different sintering mechanisms. The first one is the constitutive law developed by Du and Cocks [7] for alumina powder compacts which sinter by solid-state diffusion:

$$\dot{\varepsilon}_{ij} = \frac{\dot{\varepsilon}_0}{\sigma_0}\left(\frac{d_0}{d}\right)^3\left(\frac{3}{2}c(D)\,s_{ij} + 3f(D)\,(\sigma_m - \sigma_s)\,\delta_{ij}\right) \tag{16}$$

Table 1
Parameters used in the constitutive laws

σ_0 (MPa)	3.33
$\dot{\varepsilon}_0$ ($\times 10^{-4}\,\text{s}^{-1}$)	4.53
$\dot{d}_0$ ($\times 10^{-10}\,\text{m s}^{-1}$)	7.48
σ_s (MPa)	1

in which d_0 and d represent the initial and current grain-size, respectively, $\dot{\varepsilon}_0$ is the strain rate experienced by a fully dense material of grain-size d_0 at a constant uniaxial stress σ_0, and the two functions c and f are dependent on the initial and current relative densities, D_0 and D:

$$f(D) = \begin{cases} \dfrac{0.54(1 - D_0)^2}{D(D - D_0)^2}, & D \le 0.95 \\ \dfrac{3.2(1 - D_0)^{1/2}}{D}, & D > 0.95 \end{cases} \tag{17}$$

and

$$c(D) = \begin{cases} \dfrac{1.08(1 - D_0)^2}{D(D - D_0)^2}, & D \le 0.95 \\ \dfrac{1}{1 - 2.5(1 - D)^{2/3}}, & D > 0.95 \end{cases}. \tag{18}$$

In this model, Possion's ratio is zero (or $\lambda = 0$) if the relative density is smaller than 0.95, which means $\zeta = 0$ and the DFEM should be valid until the relative density reaches 0.95. Du and Cocks also suggested the following law for grain-growth [7]:

$$\dot{d} = \dot{d}_0\frac{(d_0/d)^3}{(1 - D)^{2/3}}. \tag{19}$$

The parameters in Eqs. (16) and (19), i.e., σ_0, $\dot{\varepsilon}_0$, $\dot{d}_0$ and σ_s, used by Du and Cocks [7] are provided in Table 1 which are used in this paper. The free shrinking rate $\dot{\varepsilon}_{\text{exp}}$ from the Du and Cocks model can be calculated as

$$\dot{\varepsilon}_{\text{exp}} = -3\frac{\dot{\varepsilon}_0}{\sigma_0}\left(\frac{d_0}{d}\right)^3 f(D)\sigma_s. \tag{20}$$

The second constitutive law used here is that developed by Olevsky [8] which is give by

$$\dot{\varepsilon}_{ij} = \frac{s_{ij}}{2\eta_s} + \frac{\sigma_m}{3\eta_B}\delta_{ij} - \frac{\sigma_s}{3\eta_B}\delta_{ij} \tag{21}$$

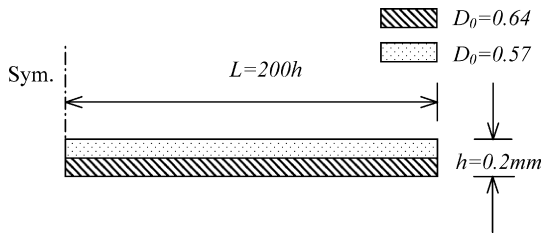

Fig. 1. Case study A—a film consisting of two perfectly bounded porous layers of different initial densities is sintered as the temperature rises from 30 to 1000 °C and is held at 1000 °C. Only half of the problem is modelled due to symmetry. The plane stress condition is assumed.

in which

$$\eta_S = D^2\eta_0 \tag{22}$$

and

$$\eta_B = \frac{2D^3}{3(1-D)}\eta_0. \tag{23}$$

Eqs. (22) and (23) lead to an expression for the viscous Possion's ratio of $\nu = (3D-1)/(3D+1)$, which takes the value from 0.315 to 0.5 as the relative density varies from 0.64 to 1. Therefore Olevsky's constitutive law certainly violates the condition of $\lambda = 0$. The free shrinking rate $\dot{\varepsilon}_{exp}$ corresponding to Olevsky's constitutive law is simply given by

$$\dot{\varepsilon}_{exp} = -\frac{\sigma_s}{3\eta_B}. \tag{24}$$

The sintering stress σ_s is taken as 1 MPa in all the following case studies.

3.1. Case A: sintering of a bi-layer film

First we consider the sintering of a film consisting of two porous layers of different relative densities of 0.64 and 0.57, respectively, as shown in Fig. 1. Each layer has a uniform material property and the two layers have the same thickness. The sintering temperature is raised from 30 to 1000 °C during a time period of 300 s in the case of solid-state sintering (the Du and Cocks model) and 600 s in the case of viscous sintering (the Olevsky model), and then held at 1000 °C. In this case study the parameters $\dot{\varepsilon}_0$ and η_0 in the two constitutive laws are taken as

$$\dot{\varepsilon}_0\,(s^{-1}) = 4.53\times10^{-4}\,\frac{\exp(-350/8.31447\,T)}{\exp(-350/8.31447\,T_{max})} \tag{25}$$

and

$$\eta_0\,(Pa\,s) = 5.0\times10^{-7}\exp\left(-\frac{350}{8.31447\,T}\right) \tag{26}$$

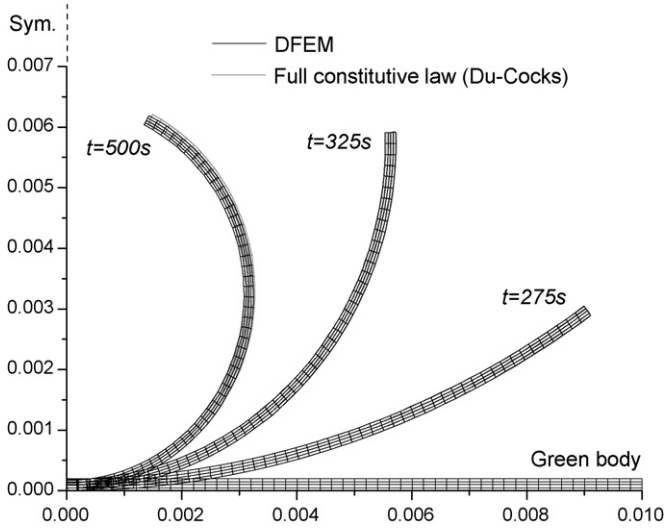

Fig. 2. Comparison between the DFEM and full FEM solutions for case study A at different times of sintering for solid-state sintering using the constitutive law due to Du and Cocks.[7]

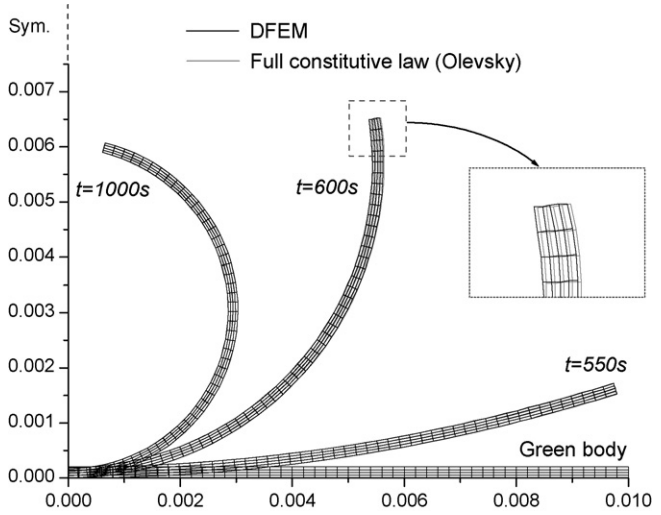

Fig. 3. Comparison between the DFEM and full FEM solutions for case study A at different times of sintering for viscous sintering using the constitutive law due to Olevsky.[8]

in which T_{max} is the holding temperature. During sintering the film warps to form an arc-shape because the two layers have different shrinkages. This is a very sensitive case—small deformations accumulate to give a large deflection at the free end of the film. In the numerical analysis, a small difference in the velocity field can therefore lead to a large difference in the displacement at the free end. The case is an ideal benchmark to test the validity of the DFEM. In the finite element model, the problem is treated as a plane stress problem and a total number of 200 eight-noded quadratic elements are used for half of the film due to symmetry. Fig. 2 shows the comparison between the finite element solution obtained using the constitutive law by Du and Cocks and the corresponding DFEM solution. Fig. 3 shows the comparison between the finite element solution obtained using the constitutive law by Olevsky and the corresponding DFEM solution. It can be observed from the two figures that the DFEM works so well that the difference between the two solutions is

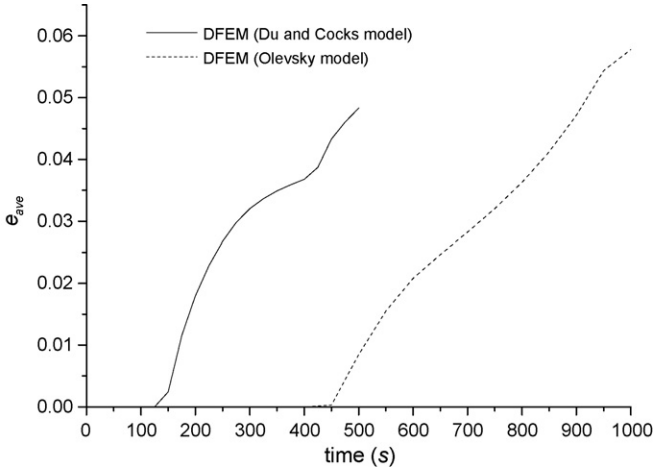

Fig. 4. The error estimator, e_{ave}, as functions of time for the cases shown in Figs. 2 and 3. The small values of e_{ave} indicate that the DFEM is valid for the entire shape evolution for both cases.

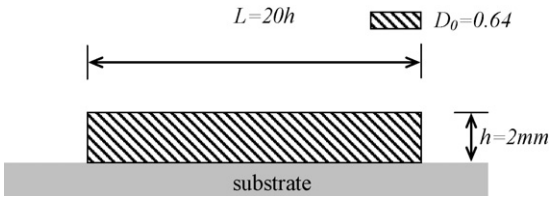

Fig. 5. Case study B—a single layer of porous film is perfectly bounded to a rigid substrate and sintered at a constant temperature. The plane strain condition is assumed (no shrinkage normal to the paper).

difficult to discern. A locally enlarged comparison is therefore provided in Fig. 3 at $t = 600$ s. Fig. 4 shows the values of the error estimator, $e_{\text{ave}}(t)$, as functions of time for the two cases. It can be seen that the good agreement between the DFEM and the FEM solutions is reflected by the error estimator. It is interesting to note that the DFEM works well even for the viscous sintering case as λ is far from zero in this case.

3.2. Case B: sintering of a single layer of thin film on a rigid substrate

Next we consider a single porous layer perfectly attached to a rigid substrate as shown in Fig. 5. In the finite element model a total number of 108 eight-noded elements were used for half of the film and a plane strain condition is assumed to simulate surface coating. Constant values of $\eta_0 = 1.0 \times 10^8$ Pa s and $\dot{\varepsilon}_0 = 4.53 \times 10^{-4}\ \text{s}^{-1}$ were used in this case study. Fig. 6 compares the DFEM solution with the full finite element solution for (a) Du and Cocks model without grain-growth, (b) Du and Cocks model with grain-growth and (c) Olevsky model. The initial profile of the film (green body) is shown using the dashed lines. The sintering times at which the comparisons are made are chosen such that the same material in free sintering would have reached the full density. In the case with grain-growth (Fig. 6(b)), the grain-size increased from the initial 0.3 to 0.9 μm at the time of the comparison. It can be observed from Fig. 6 that the DFEM and the FEM solutions agree very well with each other for all the three cases. However, the DFEM works less well when the two solutions are compared at an intermediate sintering time of $t = 600$ s as shown in Fig. 7. Again this is reflected in the values of the two error estimators. The values of e_{ave} for the two cases are about 1.8. However the value of e_{var} is small for both cases as shown in Fig. 8 . This indicates that the DFEM should be valid for predicting the final deformation but less accurate to predict the intermediate deformation, in agreement with what is shown in Figs. 6 and 7.

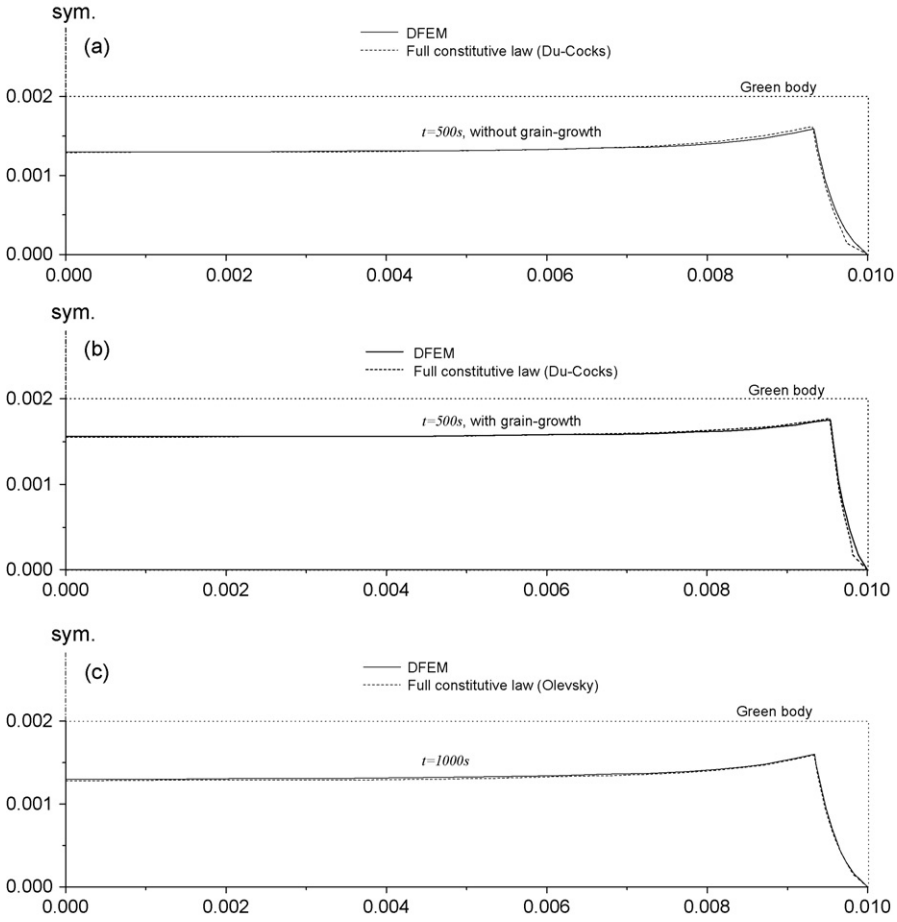

Fig. 6. Comparison between the DFEM and FEM solutions for case study B assuming: (a) solid-state sintering using the constitutive law due to Du and Cocks [7] without grain growth, (b) solid-state sintering using the constitutive law due to Du and Cocks [7] with grain growth, and (c) viscous sintering using the constitutive law due to Olevsky.[8]

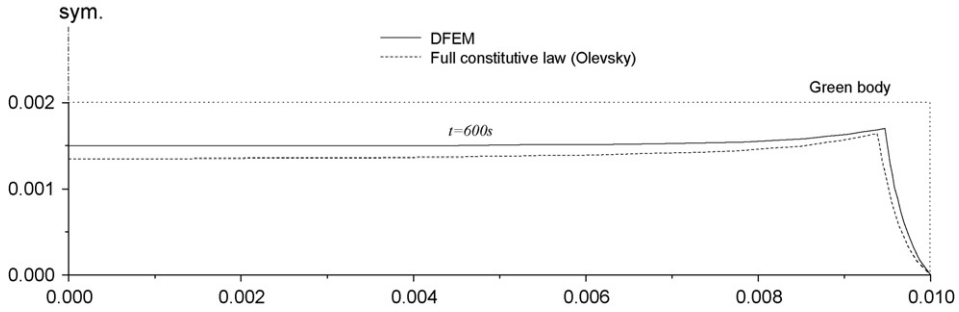

Fig. 7. Comparison between the DFEM and FEM solutions at an intermediate sintering time for case study B assuming viscous sintering using the constitutive law due to Olevsky.[8]

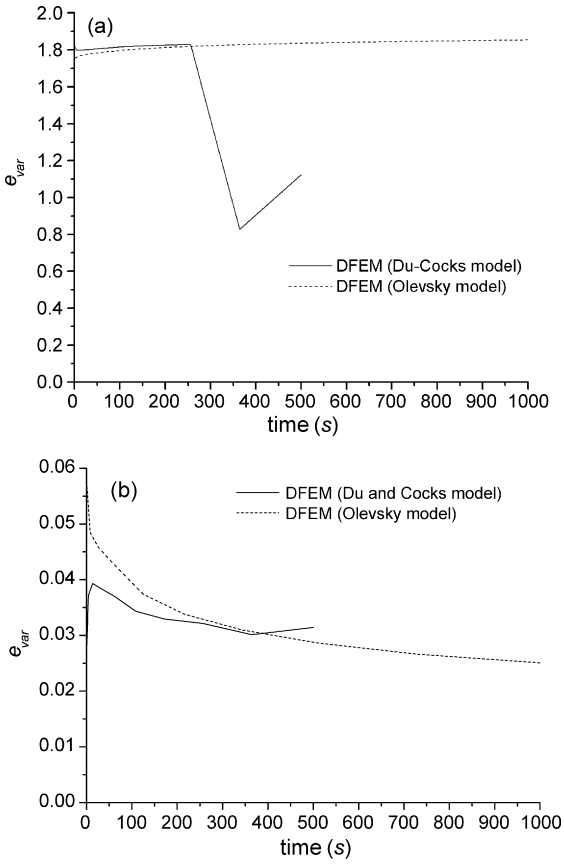

Fig. 8. The error estimators, e_{ave} and e_{var}, as functions of time calculated from the DFEM solutions shown in Fig. 6(a) and (c), respectively. The relatively large values of e_{ave} and small values of e_{var} indicate that the DFEM solutions are accurate in predicting the final deformation but less accurate in predicting the intermediate deformation.

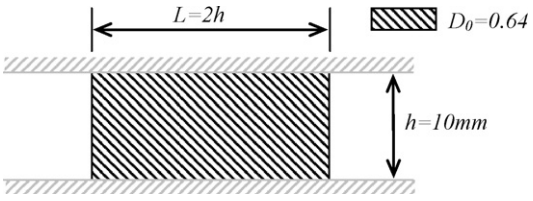

Fig. 9. Case study C—a heavily constrained case in which the upper and lower boundaries are completely fixed and the plane strain condition is enforced. Only the left and right boundaries can deform.

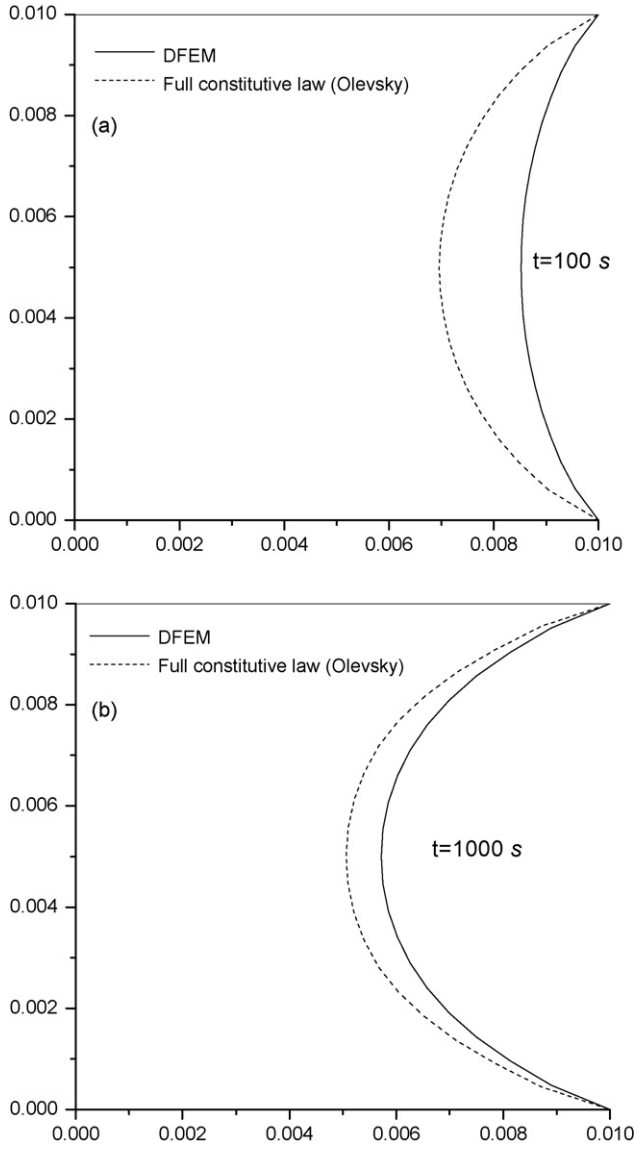

Fig. 10. Comparison between the DFEM and FEM solutions for case study C at (a) $t = 100$ s and (b) $t = 1000$ s. Olevsky's constitutive law [8] was used in this case study.

3.3. Case C: sintering between two rigid constraints

We would like to find a case in which the DFEM is completely invalid. Fig. 9 shows a severely constrained case in which the upper and lower boundaries of a rectangular porous sample are completely fixed. A plane-strain condition is enforced so that there is no shrinkage normal to the paper. Only the left and right boundaries are free to deform. The dimensions and the initial density of the sample are shown in the figure. The problem is analysed firstly using Olevsky's constitutive law with $\eta_0 = 1.0 \times 10^8$ Pa s and $\sigma_s = 1$ MPa, and then using the reduced method. Fig. 10 shows the comparison between the two solutions at $t = 100$ s (Fig. 10(a)) and $t = 1000$ s (Fig. 10(b)), respectively. It is worth to note that the material would have reached its full density at $t = 1000$ s if it was sintered freely. It can be seen that the DFEM solution significantly lags behind the full solution but still approaches the full solution as sintering proceeds. The two solutions would finally converge if the simulation is further continued. This behaviour of the DFEM solution is clearly reflected by the values of the two error estimators, e_{ave} and e_{var}, as shown in Fig. 11(a) and (b). The value of e_{ave} is large indicating that the DFEM solution differs from the full solution at the intermediate stage of sintering, but the value of e_{var} is relatively small indicating that the two solutions converge as the sample continue to sinter.

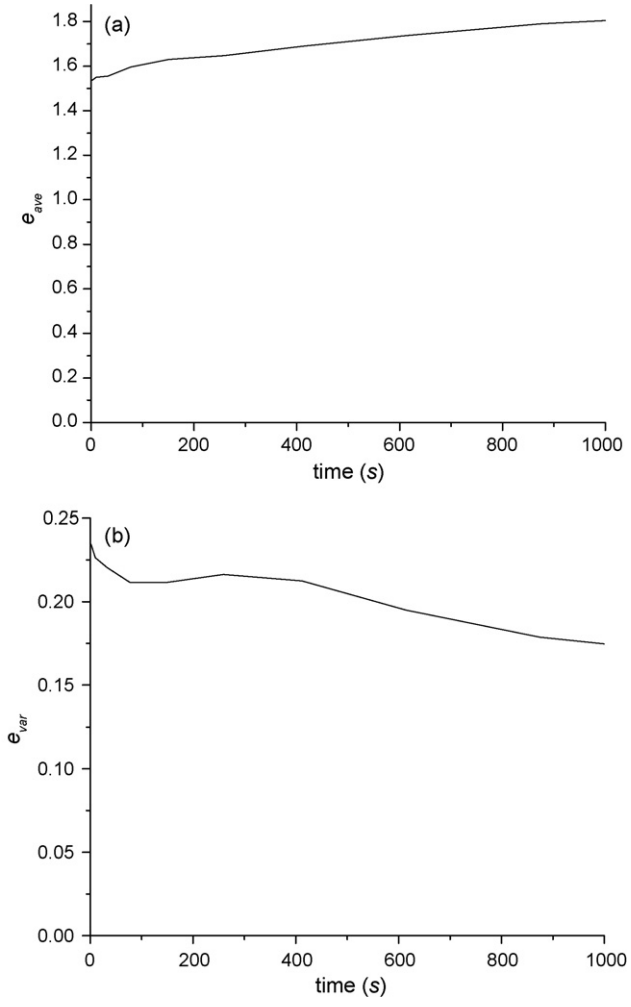

Fig. 11. Error estimators, e_{ave} and e_{var}, as functions of time calculated from the DFEM solution shown in Fig. 10. The relatively large values of e_{ave} show that the DFEM solution is poor in predicting the intermediate deformation. The reasonably small values of e_{var} indicate that the DFEM can predict the final deformation fairly well.

3.4. Case D: sintering of triple layers of thin film on a rigid substrate

Finally we present some sophisticated cases of three layers of porous films perfectly bounded to each other and to a rigid substrate as shown in Fig. 12. The total thickness and width of the films are the same as those in case B. The top and bottom layers are taken as the same material while the middle layer has a different initial property. Three different cases are considered as shown in Fig. 12: (a) the middle layer has a high initial density; (b) the middle layer has a low initial density; (c) the middle layer has a different initial grain-size. Constant values of $\eta_0 = 1.0 \times 10^8$ Pa s and $\dot{\varepsilon}_0 = 4.53 \times 10^{-4}\ s^{-1}$ are used in this case study. Fig. 13 compares the full finite element solutions with corresponding DFEM solution for five different cases. Figures (a–c) in Fig. 13 correspond to cases (a–c) shown in Fig. 12. Figures (d) and (e) correspond to cases (a) and (b) in Fig. 12. The times of comparison are chosen such that the layer with the lowest initial density would have reached full density in free sintering. It can be seen that in all the cases, the DFEM and the full solutions are in fairly well agreement for all the cases.

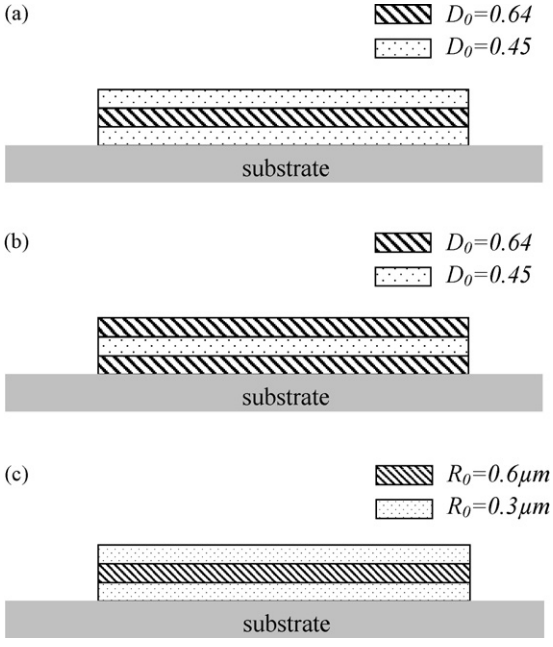

Fig. 12. Case study D—three different triple layers of films on a rigid substrate are sintered at a constant temperature. The plane strain condition is assumed.

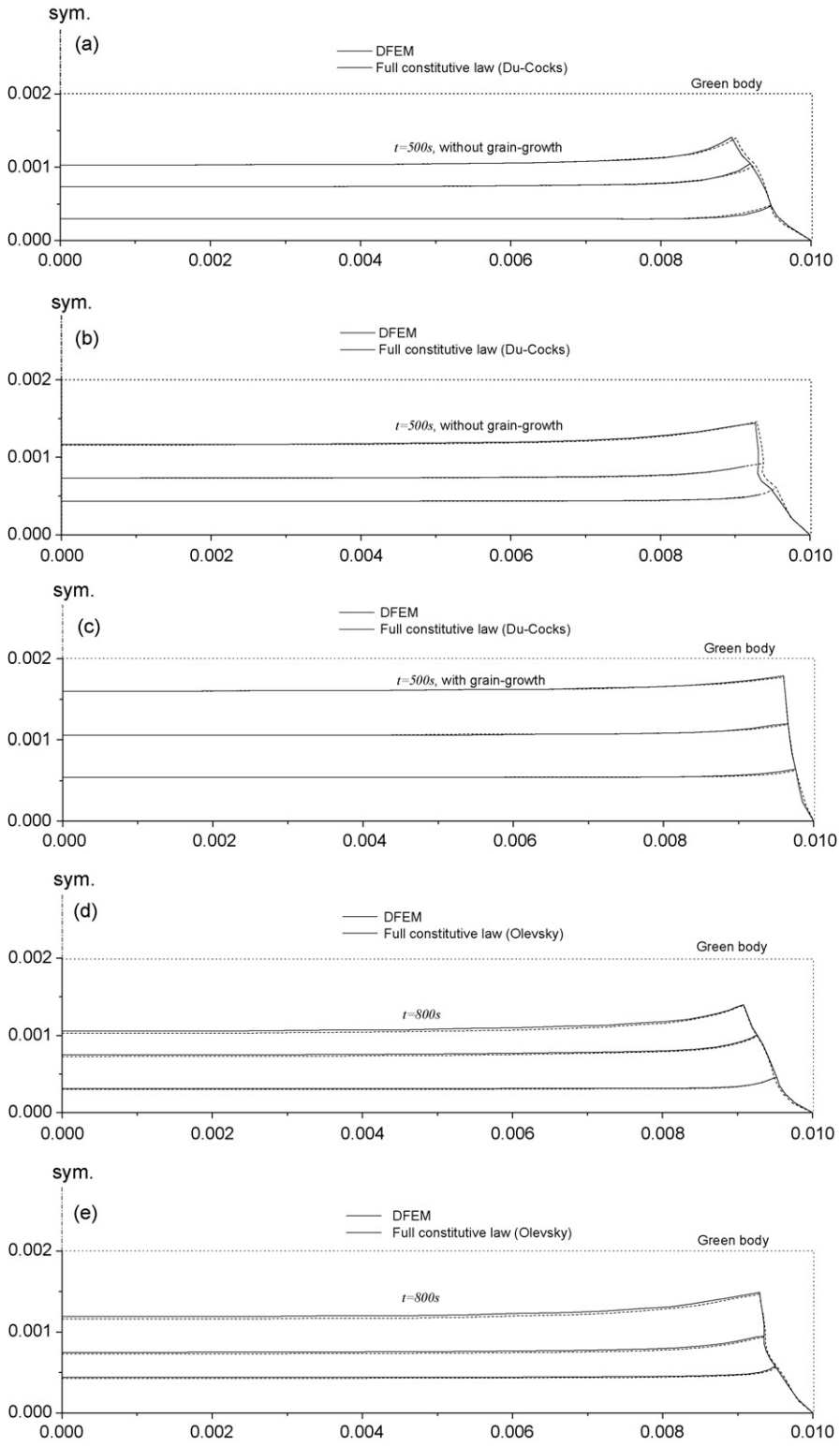

Fig. 13. Comparisons between the DFEM and FEM solutions for case study D: (a) case shown in Fig. 12(a) assuming solid-state sintering; (b) case shown in Fig. 12(b) assuming solid-state sintering; (c) case shown in Fig. 12(c) assuming solid-state sintering with grain growth; (d) case shown in Fig. 12(a) assuming viscous sintering; and (e) case shown in Fig. 12(b) assuming viscous sintering.

4. Concluding remarks

The DFEM can be used to predict the shape evolution of constrained multi-layered films during sintering. Because the reduced method only requires the densification data, instead of the full constitutive law, it can be conveniently used in a proof of concept analysis when designing sophisticated multi-layered systems, oxide fuel cells for example. The error estimators pro-

posed in this paper make it possible to determine if a DFEM analysis is valid in comparison with a finite element analysis using a full constitutive law after the analysis without knowing the constitutive law. As a note of caution, it is important to point out that the constrained layers may behave anisotropically during sintering and that anisotropy is not included in the current DFEM formulation. It is possible to include the anisotropic behaviour by replacing $\dot{\varepsilon}_{\text{exp}}$ in Eq. (2) with a set of anisotropic rates which is a work undergoing.

Acknowledgement

This work is supported by an EPSRC research grant S97996 which is gratefully acknowledged.

References

1. Gillia, O., Phenomenological modelling of the behaviour of sintering materials and numerical modelling of industrial sintering of cemented carbide and alumina (modelisation phenomenologique du comportment des materiaux frittants et simulation numerique du frittage industriel de carbure cemente et d'alumine), PhD Thesis, Institut National Polytechnique De Grenoble, France, January 2000.
2. Gillia, O., Josserond, C. and Bouvard, D., Viscosity of WC–Co compacts during sintering. *Acta Mater.*, 2001, **49**, 1413–1420.
3. Kim, H. G., Gillia, O., Doremus, P. and Bouvard, D., Near net shape processing of a sintered alumina. *Int. J. Mech. Sci.*, 2002, **44**, 2523–2539.
4. Kim, H. G., Gillia, O. and Bouvard, D., A phenomenological constitutive model for sintering of alumina powder. *J. Eur. Ceram. Soc.*, 2003, **23**, 1675–1685.
5. Raether, F., Hofmann, R., Müller, G. and Sölter, H. J., A novel thermo-optical measuring system for the in situ study of sintering processes. *J. Therm. Anal.*, 1998, **53**, 717–735.
6. Kiani, S., Pan, J., Yeomans, J. A., Barriere, M. B. and Blanchart, P., Finite element analysis of sintering deformation using densification data instead of a constitutive law. *J. Eur. Ceram. Soc.*, 2007, **27**, 2377–2383.
7. Du, Z. Z. and Cocks, A. C. F., Constitutive models for the sintering of ceramic components. I. Material models. *Acta Metal.*, 1992, **40**, 1969–1972.
8. Olevsky, E. A., Theory of sintering: from discrete to continuum. *Mater. Sci. Eng.*, 1998, **R23**, 41–100.